Picosecond studies of excitation transport in a finite volume: The clustered transport system octadecyl rhodamine B in triton X-100 micelles

M. D. Ediger, R. P. Domingue, and M. D. Fayer
Department of Chemistry, Stanford University, Stanford, California 94305

(Received 15 June 1983; accepted 20 October 1983)

A detailed experimental and theoretical examination of electronic excited state transport in the finite volume system, octadecyl rhodamine B molecules in triton X-100 micelles, is presented. Picosecond fluorescence mixing and transient grating techniques were used to examine systems in which the average number of chromophores per micelle ranged from 0.1 to 11. Because of the clustering of chromophores in the small micelles, the energy transport observed is extremely efficient. A statistical mechanical theory, based on a density expansion with a Padé approximant, is developed for donor–donor transport on a spherical surface. This theory accurately accounts for the experimental data with only the micelle radius as an adjustable parameter. The radius obtained from this procedure is in good agreement with determinations by other methods. This demonstrates that quantitative information about the spatial extent of chromophore distributions in small volumes can be obtained when appropriate finite volume energy transport theories are employed. It is shown that theories developed for infinite volumes are not applicable to systems such as the ones considered here. Finally the partitioning of rhodamine B and octadecyl rhodamine B between aqueous and micellar phases is measured, and lifetimes and rotation times are reported.

I. INTRODUCTION

Electronic excitation transport among molecules randomly distributed in solution has been actively studied recently both theoretically and experimentally. These studies of donor to donor transport[1–6] or donor transport with trapping[7,8] have focused on infinite volume systems with an infinite number of particles (the thermodynamic limit). There are a variety of experimental situations in which transport occurs where the volume or the number of chromophores involved may be too small to allow the application of infinite volume solution theories. Examples of these are chromophores attached to an isolated polymer coil[9–11] and photosynthetic antenna complexes.[12,13]

In this paper we present picosecond transient grating and fluorescence mixing experiments on excitation transfer among donors randomly distributed at the surface of Triton X-100 micelles, and we develop a theory which accurately accounts for the experimental data. Micelles have been extensively studied and their physical properties are relatively well understood. As such, they present a good physical situation for testing energy transport theories for finite volumes. Although energy transfer in finite volume systems has been studied by other workers,[14–18] these approaches have concentrated on donor–trap transfer where donors are dilute enough to be considered noninteracting. Our main interest in this paper will be the accurate description of donor–donor transport in a finite system.

Donor–donor transfer makes possible the efficiency of light-harvesting finite volume systems in nature.[13] Many interacting donors must be present in order to assure that a photon captured somewhere in the system is transported to a trap (reaction center). Likewise, in any attempt to mimic nature in this respect, systems of many donors and few traps are likely to be utilized. As in nature, clustering the donors in a small volume about the trap is necessary for efficient light harvesting by an artificial reaction center or a specialized fluorescent center.[19] Thus understanding donor–donor transport dynamics in finite volume systems is important for both practical and fundamental scientific reasons.

Results for rhodamine B (RB) and octadecyl rhodamine B (ODRB) in aqueous Triton X-100 micelle solutions are presented below. Even in solutions with low chromophore concentrations where no energy transport can occur, a large fraction of the RB remains in the water and is not associated with a micelle. The RB in the water not only makes energy transport inefficient, but the fast rotation time of the aqueous RB masks the energy transport dynamics of the micellar RB. The lifetime and rotation time of RB and the partitioning between water and micelles are given for several concentrations.

The long hydrocarbon tail of ODRB increases the solubility of the chromophore in the micelle to such an extent that virtually every ODRB molecule is associated with a micelle. The micelle concentrations are sufficiently low that excitation transport between chromophores in different micelles is negligible. The detailed investigation of energy transport in these systems yield three basic results. (1) The statistical mechanical theory, which employs a density expansion with a Padé approximant, provides a very good description of these finite volume systems. (2) The efficiency of energy transport among donors is greatly enhanced by clustering the donors in the small volume micelle systems. (3) The energy transport measurements yield the radius of the micelles. When appropriate finite volume transport theories are utilized, energy transport experiments can provide quan-

 0021-9606/84/031246-08$02.10

titative information about the size of micelles and other finite volume systems such as isolated polymer coils.[11]

II. THEORY AND CALCULATION OF OBSERVABLES

In this section we present a model for energy transport among chromophores distributed randomly on the surface of a micelle. Our goal is to calculate $G^s(t)$, the time-dependent ensemble averaged probability that the excitation is on the originally excited chromophore in the absence of lifetime decay processes. G^s has contributions from excitations which have not left the initially excited chromophores and from excitations which have been transferred to other chromophores and then returned to the initially excited chromophores. G^s is a fundamental quantity associated with an excitation transport system, and it can be directly related to observables in a time resolved fluorescence depolarization experiment.

We consider a random distribution of N donor molecules (no traps) on a spherical shell of radius $\mathscr{R}$. G^s will be calculated using a density expansion in powers of the chromophore density with a Padé approximant. The following derivation closely follows an approach recently used by two of the authors to obtain G^s for another finite volume system. In that paper (Ref. 20, hereafter referred to as I), the chromophores were randomly distributed *within* a spherical volume. Here we will outline only the essential features of the present problem. We begin by developing an expression for $\hat{G}^s(\epsilon)$, the Laplace transform of $G^s(t)$.

The configuration of the system K is characterized by the locations of the N donor molecules, $(\mathbf{r}_1,\mathbf{r}_2,\ldots,\mathbf{r}_N)$. The probability that an excitation is found on the j th molecule for the configuration K at time t, $p_j(K,t)$, satisfies the master equation

$$\frac{dp_j(K,t)}{dt} = -\frac{p_j(K,t)}{\tau_F} + \sum_{i=1}^{N} w_{ji}\left[p_i(K,t) - p_j(K,t)\right] . \quad (1)$$

τ_F is the measured excited state lifetime and w_{ji} is the transfer rate between molecules j and i ($w_{jj} = 0$). For dipole–dipole interactions, the orientation averaged transfer rate is

$$w_{ji} = \frac{1}{\tau_F}\left(\frac{R_0^{DD}}{r_{ji}}\right)^6 , \quad (2)$$

where R_0^{DD}, the critical transfer radius for donor–donor transport, contains the strength of the interaction. (The full angular dependence of the transfer rate needs to be considered in calculating G^s for the experimental conditions utilized in this paper, i.e., the molecules have fixed orientations on the time scale of energy transfer. The connection between G^s for the orientation averaged rate and G^s for the angle dependent rate will be considered later in this section.)

After eliminating the lifetime decay term and expanding the Laplace transform of G^s in powers of the chromophore density, we obtain the following expression analogous to Eq. (17) in I[21]:

$$\hat{G}^s(N,R,\epsilon) = \frac{1}{\epsilon} - \frac{(N-1)}{A^2}\int_S d\sigma_1 \int_S d\sigma_2 \frac{w_{12}}{\epsilon(\epsilon+2w_{12})} - \frac{(N-1)(N-2)}{A^3}\int_S d\sigma_1 \int_S d\sigma_2 \int_S d\sigma_3 \times \left\{\frac{\epsilon w_{12} + w_{12}w_{13} + w_{12}w_{23} + w_{13}w_{23}}{\epsilon[\epsilon^2 + 2\epsilon(w_{12}+w_{13}+w_{23}) + 3(w_{12}w_{13}+w_{12}w_{23}+w_{13}w_{23})]} - \frac{w_{12}}{\epsilon(\epsilon+2w_{12})}\right\} . \quad (3)$$

In this equation, the integrals are surface integrals over a sphere of radius $\mathscr{R}$ and A is the surface area ($4\pi\mathscr{R}^2$). Since $\hat{G}^s(\epsilon)$ and $G^s(t)$ are functions of $\mathscr{R}/R_0^{DD}$, we have defined this dimensionless radius as R and have indicated this dependence explicitly in the equation above.

The two integrals in Eq. (3) can be written as functions of one dimensionless parameter

$$\alpha = R^2\left(\frac{\epsilon\tau_F}{2}\right)^{1/3} . \quad (4)$$

Hence the previous equation can be written as

$$\hat{G}^s(N,R,\epsilon) = \frac{1}{\epsilon}\left[1 - \frac{(N-1)}{\alpha}h_2(\alpha) + \frac{(N-1)(N-2)}{\alpha^2}h_3(\alpha)\right] . \quad (5)$$

All the information about the effects of the finite volume are contained in $h_2(\alpha)$ and $h_3(\alpha)$. $h_2(\alpha)$ can be evaluated analytically:

$$h_2(\alpha) = \frac{1}{48}\left\{\ln\left[\frac{(4\alpha+1)^2}{(16\alpha^2-4\alpha+1)}\right] + 2\sqrt{3}\left[\arctan\left(\frac{8\alpha-1}{\sqrt{3}}\right) + \frac{\pi}{6}\right]\right\} , \quad (6)$$

$h_3(\alpha)$ reduces to a three-dimensional numerical integral which has been fit to analytical functions presented in Appendix A.

Equation (5) is the exact solution of the energy transport problem of up to three molecules randomly distributed on a spherical surface. It is a good approximation at short times when $N > 3$. In order to develop a better approximation to $\hat{G}^s(N,R,\epsilon)$ for $N > 3$, we follow I in rewriting Eq. (5) as

$$\hat{G}^s(N,R,\epsilon) = \epsilon^{-1}\left\{1 + \frac{(N-1)}{\alpha}h_2(\alpha) + \frac{(N-1)^2}{\alpha^2}\left[(h_2(\alpha))^2 - \left(\frac{N-2}{N-1}\right)h_3(\alpha)\right]\right\}^{-1} . \quad (7)$$

Equation (7) is equal to Eq. (5) to order ϵ^{-2} when α is large, and is a Padé approximant of Eq. (5) in this limit. Equation (7) is a much better approximation to $\hat{G}^s(N,R,\epsilon)$ for $N > 3$ because it has the proper asymptotic behavior for large N and small ϵ.

In I, it was shown that the equation analogous to Eq. (7) is a very good approximation to the exact $\hat{G}^s$. We employed several of the same tests to check Eq. (7). Additionally, we used a computer simulation which picked a configuration at random, numerically solved the master equation, and ob-

tained G^s for a particular time. Results from successive runs were averaged and this process was repeated until G^s converged. Simulations were performed for systems of 4, 5, and 9 particles. These comparisons indicate that the inverse Laplace transform of Eq. (7) is essentially exact at short times (± 0.01 for $G^s > 0.7$) and in error by a maximum of 0.04 at long times.

$G^s(N,R,t)$ is easily obtained by numerical inversion of the Laplace transform.[22] In Fig. 1, we show a series of calculated curves for 1–15 donors randomly distributed on a spherical shell of $\mathscr{R} = 0.78\, R_0^{DD}(\gamma_2)^{1/2}$. The factor $(\gamma_2)^{1/2}$ is discussed below and arises from the correct consideration of the angular dependence of the transfer rate. (This value of $\mathscr{R}$ is the best fit to the experimental data presented in Sec. IV.) For this figure and for all subsequent calculations, we used Eq. (5) for $N \leqslant 3$ and Eq. (7) for $N > 3$. Note that loss of probability on the initially excited chromophore due to the excited state lifetime is not included in G^s.

We now wish to calculate the observables for the fluorescence depolarization experiment. We assume the following: all dye molecules are associated with a micelle, the dye molecules are distributed among the micelles according to a Poisson distribution, the dye molecules are randomly distributed and randomly oriented at the micelle surface, and the micelles are spherical and monodisperse in size. We want to calculate $I_\parallel(t)$ and $I_\perp(t)$, the decay of the fluorescence polarized parallel and perpendicular to the excitation polarization, respectively. We can write

$$I_\parallel(t) = e^{-t/\tau_F}[1 + 2C\phi(t)]\,, \tag{8}$$

$$I_\perp(t) = e^{-t/\tau_F}[1 - C\phi(t)]\,, \tag{9}$$

where C is a constant $\leqslant 0.4$ which describes the degree of photoselection for the transition involved. $\phi(t)$ contains all sources of depolarization, in this case, energy transport and molecular rotation. Since the rotation observed in these experiments is very slow compared to energy transfer, $\phi(t)$ can be written as follows:

$$\phi(t) = e^{-t/\tau_R}\langle G^s(N,R',t)\rangle\,. \tag{10}$$

Here τ_R is the rotational correlation time and the prime on R indicates that G^s is to be calculated with the orientation dependent transfer rate. The brackets imply a weighted average over the Poisson distribution:

$$\langle G^s(N,R',t)\rangle = \sum_{N=0}^{\infty} \frac{N}{\mu}\left(\frac{e^{-\mu}\mu^N}{N!}\right) G^s(N,R',t)\,. \tag{11}$$

μ is the average number of dye molecules in a micelle (μ = dye concentration/micelle concentration).

We need G^s for the orientation dependent transfer rate. In Appendix B, we show that within the accuracy of the theoretical development, this can be obtained from G^s for the orientation averaged transfer rate by replacing R with

$$R' = (\gamma_2)^{-1/2}R\,, \tag{12}$$

i.e.,

$$G^s(N,R',t) = G^s(N,R(\gamma_2)^{-1/2},t)\,, \tag{13}$$

where $\gamma_2 = 0.8468$. Combining Eqs. (10)–(13), we can write

$$\phi(t) = e^{-t/\tau_R}\sum_{N=0}^{\infty} \frac{N}{\mu}\left(\frac{e^{-\mu}\mu^N}{N!}\right) G^s(N,R',t) \tag{14}$$

thus allowing the calculation of $I_\parallel(t)$ and $I_\perp(t)$.

In order to directly compare the experimental $I_\parallel(t)$ and $I_\perp(t)$ with our calculations, we need to convolve the calculated $I_\parallel(t)$ and $I_\perp(t)$ with the excitation pulse $[I_e(t)]$ and the summing pulse $[I_s(t)]$ used in the fluorescence mixing experiments.[3] When the excitation pulse is much shorter than the summing pulse (as in our experiments below), an extremely accurate approximation to the true convolution equation is the convolution of $I_\parallel(t)$ or $I_\perp(t)$ with $I_{cc}(t)$, the cross correlation or convolution of $I_e(t)$ and $I_s(t)$. This is the procedure employed in the data analysis.

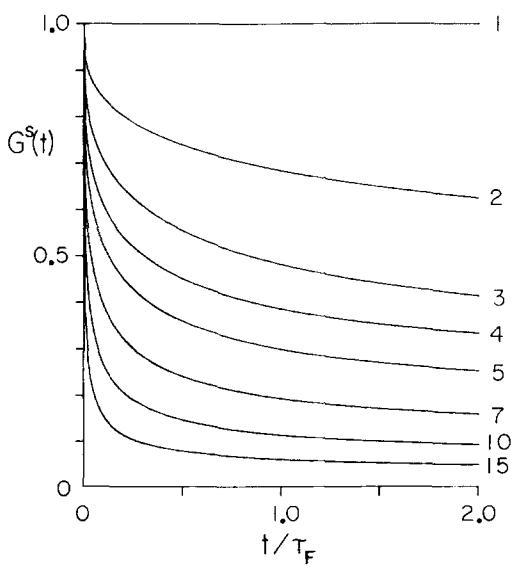

FIG. 1. $G^s(t)$, the probability that the excitation is on the originally excited molecule, for 1–15 donor chromophores randomly distributed on a sphere of radius $\mathscr{R} = 0.78\, R_0^{DD}(\gamma_2)^{1/2}$. This value of R is used in the data analysis, and γ_2 ($= 0.8648$) arises from consideration of the orientation dependent transfer rate. (See the text.) As the number of donors increases on a sphere of constant size, $G^s(t)$ decays faster. Time is in units of τ_F, the excited state lifetime. [Note that $G^s(t)$ does not include lifetime decay. The curve for one donor, since there is no energy transport, has $G^s(t) = 1$ for all times.]

III. EXPERIMENTAL METHODS

Time-resolved measurements were performed with two different techniques. Transient grating experiments (time resolution ~ 35 ps) were used to examine solutions of rhodamine B in aqueous Triton X-100. The experimental apparatus has been fully described elsewhere.[23] Fluorescence mixing experiments were used to investigate micellar solutions of octadecyl rhodamine B. The experimental apparatus is illustrated schematically in Fig. 2. The 1.06 μm output of a continuously pumped acousto-optically Q-switched and mode-locked Nd:YAG laser was frequency doubled, and the 532 nm component, a train of about 40 pulses, was used to synchronously pump a rhodamine 6G dye laser. Operating at 400 Hz, the dye laser was cavity dumped, resulting in a single pulse at 562 nm (spectral width ~ 6 cm^{-1}, FWHM = 35 ps) of about 15 μJ. This single pulse was attenuated to ~ 0.5 μJ and focused on the sample with a 700 μm spot size. The resulting fluorescence was filtered to remove scattered excitation light and focused into an RDP type-I

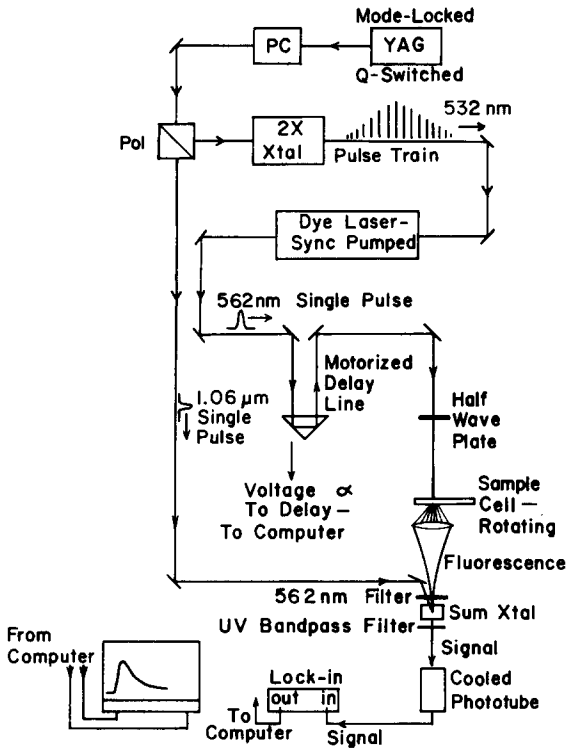

FIG. 2. Fluorescence mixing experimental setup: PC = Pockels cell; Pol = polarizer. The sample is excited by a variably delayed dye laser pulse. The resulting fluorescence is summed with a 1.06 μm pulse which provides the time resolution. The resulting short pulse of UV light is detected by a phototube and lock-in amplifier. The polarization of the exciting light is varied by the half-wave plate permitting examination of $I_{\parallel}(t)$ and $I_{\perp}(t)$.

sum-generating crystal where it overlapped with the path of a 1.06 μm single pulse ($\sim 15\,\mu$J, FWHM = 160 ps) selected from the YAG laser pulse train by a Pockels cell and polarizer. The fluorescence reaching the sum crystal coincident in time with the 1.06 μm pulse mixed with that pulse to produce a short burst of UV light (~ 380 nm). The UV intensity is proportional to the fluorescence intensity at that time. The sum crystal was oriented so that only the component of the fluorescence polarized parallel to the 1.06 μm polarization summed. A half-wave plate was used to vary the polarization of the excitation pulse relative to the summing pulse, allowing both $I_{\parallel}(t)$ and $I_{\perp}(t)$ to be obtained. The excited state lifetime τ_F can be determined directly by adjusting the relative polarization of the excitation and summing pulses to the magic angle (54.7°).[3,23]

The time decay was swept out by varying the delay between the excitation pulse and the summing pulse with a motorized delay line. The signal was detected through a UV bandpass filter by a cooled photomultiplier (EMI 6256). The phototube output was measured with a lock-in amplifier operating at the laser frequency. The lock-in output and a voltage proportional to the delay time were digitized and stored on disk.

Each sweep of the delay line took about 10 min. Several sweeps for each polarization were recorded, checked for reproducibility, and then averaged to improve the signal-to-noise ratio. As discussed in Ref. 23, the method of data acquisition preserves the relative strengths of the $I_{\parallel}(t)$ and $I_{\perp}(t)$ curves, so that their ratio is known absolutely.

The samples consisted of known concentrations of rhodamine B (Exciton) and octadecyl rhodamine B chloride (Molecular Probes) in aqueous solutions of Triton X-100 (Baker). The rhodamine B solutions were basic to assure that only one form of the molecule was present. The octadecyl rhodamine B(ODRB) solutions had pH$\sim$7. The sample holder was a rotating cell of 5 cm diameter formed by two optical flats separated by spacers (3 μm to 1 cm). The maximum OD was lowered until no reabsorption could be observed in the detected signal (OD < 0.08). Likewise, the excitation pulse was attenuated until saturation and stimulated emission were eliminated. All experiments were performed at 21.5 ± 1.0 °C.

R_0^{DD} for ODRB was determined by the spectral overlap method of Förster.[24] Fluorescence spectra of ODRB were recorded and digitized with a computer interfaced SPEX 1702 1 m monochromator and an EMI 9658 photomultiplier. Corrections were made for the monochromator and photomultiplier wavelength response using a blackbody lamp of known color temperature. Disodium fluorescein (Exciton) in 0.1 N NaOH was used as a quantum yield standard.[25] Low OD fluorescence samples were excited by the vertically polarized 514.5 nm line of an Ar^+ laser. Fluorescence was detected at 90°, through a polarizer set at the magic angle relative to the excitation polarization.[26] Absorption spectra of ODRB were recorded with a computer interfaced Cary 14 spectrometer. The digitized absorption and fluorescence data were used to numerically calculate the absorption–emission overlap integral, and then R_0^{DD}.

IV. RESULTS AND DISCUSSION

Previous workers have shown that xanthene dyes tend to prefer micellar environments to aqueous solution.[14,27] As a necessary precursor to the energy transport experiments, we investigated the distribution of rhodamine B (RB) molecules between water and micelles in aqueous solutions of Triton X-100. Both the lifetime and rotation time of RB depend on whether it is associated with a micelle or in free solution, and measurement of either can be used to determine the partitioning of RB between the water and the micelles.

Transient grating measurements of very dilute RB in pure water gave the aqueous phase lifetime $\tau_F(H_2O)$ and the aqueous phase rotation time $\tau_R(H_2O)$. Since the fluorescence lifetime in the micellar environment τ_F(micelle) is different than $\tau_F(H_2O)$, examination of the lifetime decay of a solution where chromophores are present in both environments yields a biexponential. Knowing $\tau_F(H_2O)$ permits an accurate determination of τ_F(micelle) and the ratio of the preexponentials. In a transient grating experiment, the fluorescence quantum yield does not enter into the ratio of the preexponentials. Since the absorption cross section is the same in both environments, the ratio of the preexponentials is the ratio of the number of chromophores in the aqueous and micellar environments. Similarly, examination of the depolarization data allows τ_R(micelle) to be calculated and gives an independent measure of the fraction of the chromophores in each environment.

Both the lifetime and rotation approaches gave similar results and the average is shown in Table I. Columns 1 and 2 give the RB and Triton X-100 concentrations, respectively. Column 3 gives the number of dye molecules that on the average would be in each micelle if the fraction of RB in the aqueous component was zero. Column 4 gives the actual fraction of RB molecules in water. Since almost half of the RB is in the water at a concentration where only very few micelles have more than one chromophore, this system is not an efficient energy transport system and is not well suited for observing the energy transport properties of interest.

To increase the affinity of the chromophore for the hydrophobic micellar environment, we employed a derivative of RB containing a long alkane chain, i.e., octadecyl rhodamine B (ODRB). Experimental evidence demonstrates that ODRB is completely associated with the micelles. ODRB in saturated aqueous solution ($<10^{-5}$ M) shows a strongly broadened absorption spectrum, a low fluorescence quantum yield (<0.05), and a very short fluorescence lifetime (<250 ps). In contrast, a similar concentration dissolved in aqueous Triton X-100 (0.5% by weight) exhibits an absorption spectrum very much like RB in organic solvents or ODRB in methanol. The quantum yield is high (0.57 ± 0.07) and the fluorescence decays exponentially with a relatively long lifetime ($\tau_F = 2.69 \pm 0.03$ ns). Additionally, the rotation time ($\tau_R = 8.1 \pm 0.3$ ns) in micellar solution is consistent with the viscous micellar medium[27] and is much different than the rotation time we measured for ODRB in methanol ($\tau_R = 223 \pm 15$ ps), which has a low viscosity like water.

The conclusion that the addition of a long alkane chain to a charged molecule like rhodamine B drives the molecules into the micellar environment is consistent with recent work by Plückthun and Dennis.[28] They found that long alkane chains on phosphatidyl choline produced complete association with Triton X-100 micelles.

Figure 3 shows the experimental $I_{\parallel}(t)$ and $I_{\perp}(t)$ for a 6.0×10^{-6} M ODRB in 0.5% Triton X-100 solution. Also on the figure are the theoretical curves calculated as described in Sec. II, using $\tau_F = 2.69$ ns, $\tau_R = 8.1$ ns, and the initial polarization anisotropy $C = 0.36$.

Since 0.5% is about 40 times the critical micelle concentration for pure Triton X-100,[29] we assume that a negligibly small amount of Triton is not involved in micelles. The micelle concentration is low enough that transport between chromophores on different micelles is negligible. On the basis of light scattering[30] and x-ray scattering experiments,[31] we take the molecular weight of a Triton micelle to be 93 000 at 21.5 °C. Thus, the data shown in Fig. 3 has the average number of chromophores per micelle $\mu = 0.11$. Energy transfer is not significant at this concentration.

TABLE I. Partitioning of rhodamine B between water[a] and Triton X-100 micelles.[b]

[RB] M	[Triton] %	$\frac{[RB]}{[micelles]}$	f_{H_2O}[c]
10^{-5}	5.0	0.02	0.25 ± 0.05
10^{-5}	0.5	0.19	0.38 ± 0.05
10^{-4}	5.0	0.19	0.29 ± 0.09

[a] $\tau_F(H_2O) = 1.67 \pm 0.06$ ns; $\tau_R(H_2O) = 0.223 \pm 0.015$ ns.
[b] τ_F(micelle) $= 3.25 \pm 0.20$ ns; τ_R(micelle) $= 5.3 \pm 1.0$ ns.
[c] f_{H_2O} = fraction of RB molecules not associated with a micelle.

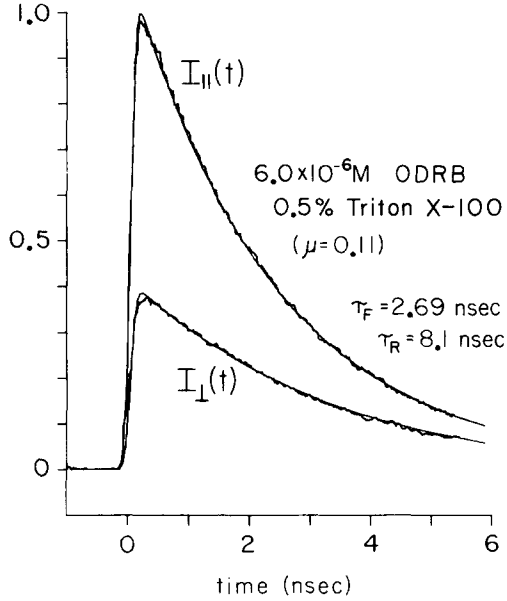

FIG. 3. Time-resolved fluorescence mixing data for a low concentration (6.0×10^{-6} M) sample of ODRB in 0.5% Triton X-100. The decay of the fluorescence polarized parallel and perpendicular to the excitation polarization is shown. The average number of chromophores per micelle $\mu = 0.11$. Hence virtually no energy transport occurs. After determining the excited state lifetime τ_F at the magic angle polarization, the rotational lifetime τ_R was obtained from $I_{\parallel}(t)$ and $I_{\perp}(t)$ (Refs. 3 and 23). The calculated curves use $\tau_F = 2.69$ ns, $\tau_R = 8.1$ ns, and the initial polarization anisotropy $C = 0.36$.

Having fit the experimental data in the absence of significant energy transfer, we now examine four solutions of successively higher chromophore concentrations (the Triton X-100 concentration was held fixed). The only parameter that we adjusted to account for the energy transport in this data was R', the dimensionless radius for the orientation dependent transfer rate. The best fit to the data was obtained with $R' = 0.78$. All theoretical curves shown in Figs. 3–5 were calculated with this value.

Figures 4(a) and 4(b) show the moderate concentration experimental data and theoretical curves for $\mu = 0.56$ and 2.2, respectively. By $\mu = 0.56$, a significant fraction of the micelles have more than one chromophore. It is clear that the theory not only accurately predicts the *shapes* of $I_{\parallel}(t)$ and $I_{\perp}(t)$, but also the relative *heights*. At $\mu = 2.2$ [Fig. 4(b)] G^s has decayed to 0.48 by 5 ns ($\sim 2\tau_F$). Thus energy transport is strongly affecting the polarized fluorescence signal. The calculated curves are quite sensitive to both the dimensionless radius R' and the average number of chromophores per micelle μ. For example, in Fig. 4(b) if $R' = 0.82$, the calculated curves do not fit the data within the noise. The μ sensitivity is indicated by the dashed curve in Fig. 4(b), which is $I_{\perp}(t)$ in the absence of energy transport (from Fig. 3).

Figures 5(a) and 5(b) show the high concentration experimental data and theoretical curves ($\mu = 5.6$ and 11.2, respectively). Here the agreement is not quite as good as for

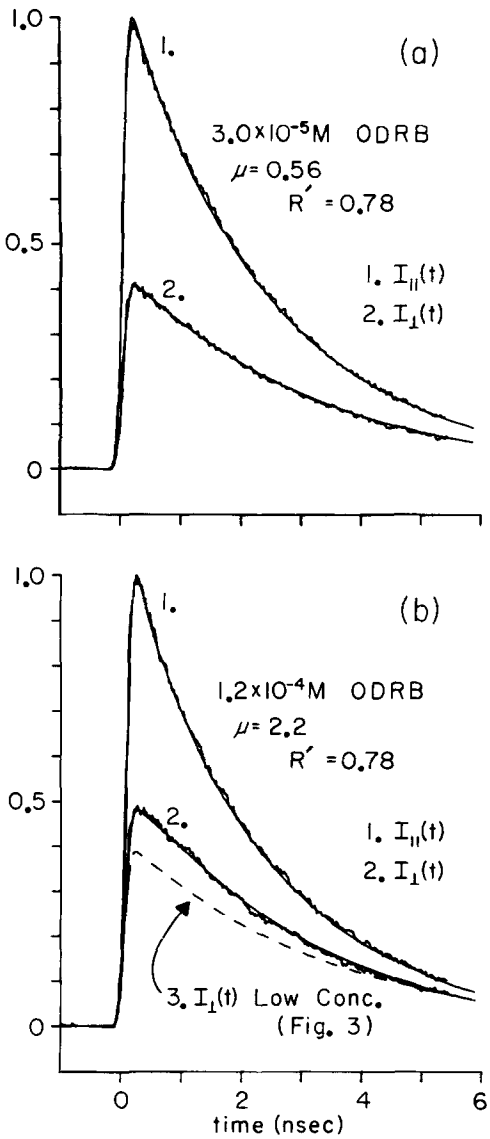

FIG. 4. Time-resolved fluorescence mixing data for (a) 3.0×10^{-5} M ODRB and (b) 1.2×10^{-4} M ODRB in 0.5% Triton. The average number of chromophores per micelle $\mu = 0.56$ and 2.2, respectively. The smooth curves running through the data were calculated using Eqs. (8) and (9). The only adjustable parameter, the dimensionless radius R', has been fixed at 0.78 for all the calculated curves in this paper. In (b), we have shown as a dashed line the calculated $I_\perp(t)$ in the absence of energy transport. This comparison demonstrates that energy transport is quite significant at $\mu = 2.2$. Note that the theory accurately predicts not only the shape of the experimental data but the relative heights of the two polarization components as well.

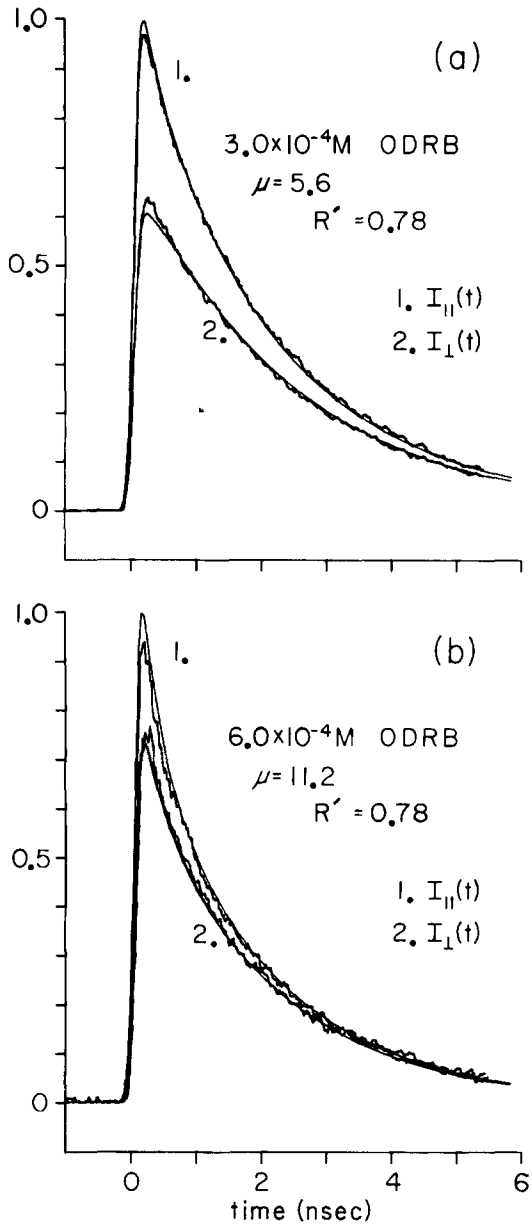

FIG. 5. Time-resolved fluorescence mixing data for (a) 3.0×10^{-4} M ODRB and (b) 6.0×10^{-4} M ODRB in a 0.5% Triton. The average number of chromophores per micelle $\mu = 5.6$ and 11.2, respectively. The smooth curves were calculated using Eqs. (8) and (9). The only adjustable parameter, the dimensionless radius R', has been fixed at 0.78 for all calculated curves in this paper. At these high concentrations, energy transport is rapid as indicated by the small difference between $I_\parallel(t)$ and $I_\perp(t)$. The discrepancies between the data and the calculated curves at these high concentrations are due to trapping by aggregates.

the lower concentrations. The deviations are explained by the existence of trapping, presumably by aggregates of ODRB within the micelles. Evidence for this is found in the lifetime decay. The lifetime decays for the three highest concentrations are somewhat faster than for the low concentrations and are no longer single exponentials. The e^{-1} points for the $\mu = 11.2$, 5.6, and 2.2 data were 1.79, 2.26, and 2.58 ns, respectively, compared to 2.69 ns at lower concentrations. [In the calculations we used the observed magic angle lifetime decay taken at each concentration to replace the exponentials in Eqs. (8) and (9). The same values of τ_R and C were used for all the calculated curves.]

Trapping by aggregates will cause G^s to decay faster and will reduce the excited state lifetime if there is enhanced radiationless decay of the trap excited state. This behavior has been observed in concentrated dye solutions in organic solvents where trapping by dimers has been shown to be responsible for fluorescence quenching.[32] The data in Fig. 5 are consistent with this observation. Notice that the theoretical fits lie above the experimental data for $I_\parallel(t)$ and below the data for $I_\perp(t)$. Examination of Eqs. (8) and (9) reveals that the experimental G^s is decaying somewhat faster than the theory predicts. This and the shortened lifetimes suggest that trapping by ODRB aggregates is involved in the highest con-

centration samples. Comparison of these results with the results for dyes in organic solvents[32] at the same local concentration indicates that aggregate quenching of excitations is less severe in the ODRB–micelle systems.

The model used in the above calculations contains several assumptions. Specifically, we wish to address the appropriateness of the Poisson distribution, the assumption that the chromophores lie near the sphere surface with random orientations, and the assumption that the micelles are spherical.

The use of the Poisson distribution to describe the chromophore distribution among the micelles presumes that the presence of one chromophore in a micelle does not affect the probability that another chromophore is present in the same micelle, i.e., the binding is neither cooperative nor anticooperative. Considering the size of the chromophore and the size of the micelle, this assumption is very reasonable as long as the mole fraction of chromophores in a micelle is small. Plückthun and Dennis[28] have shown that the Poisson distribution is accurate for phosphatidyl choline with long alkane chains in Triton X-100 micelles as long as the mole fraction is less than 0.1. (In the experiments presented here, the highest average mole fraction was 0.08.) It should be noted that for low mole fractions the Poisson distribution is very similar to the binomial distribution.

The assumption that the molecules lie near the sphere surface is based on the idea that a charged head group like the rhodamine B in ODRB should prefer a more polar environment than the hydrophobic core of the micelle. Sklar *et al.*[18] have presented experimental evidence which indicates that a similar molecule is located at the surface of lipoproteins in aqueous solution. We have also made the reasonable assumption that the chromophores are randomly oriented with respect to the surfaces and each other in the absence of more detailed knowledge.[33]

Finally, we have assumed that the Triton X-100 micelles are spherical. This is consistent with the light scattering data of Corti and Degiorgio.[30] X-ray scattering data by Paradies,[31] and calculations by Robson and Dennis[34] indicate that an oblate ellipsoid of revolution may be more realistic. Paradies determined that the long half-axes were ~ 50 Å while the short half-axis was ~ 32 Å. If the micelles are indeed somewhat nonspherical, we would expect the transport theory for spheres to fairly accurately describe the data by using some R' intermediate to the long and short half-axes. A theory of energy transfer on the surface of an ellipsoid is a straightforward extension of the current work. In spite of the disagreement over the shape of the micelles, there is agreement in the literature as to the molecular weight ($\sim 93\,000$) and the hydrodynamic radius (42 Å) at this temperature,[35] as well as the monodispersity of the micelle size.[30,31]

Assuming the micelles to be spherical, we fit our data with $R' = 0.78 \pm 0.04$. R_0^{DD} was measured spectroscopically to be 51.5 ± 1.0 Å. This implies that the micelle radius $\mathscr{R}$ equals 37 ± 2 Å, in reasonable agreement with the hydrodynamic radius reported by Corti and Degiorgio, and certainly consistent with the oblate ellipsoid dimensions reported by Paradies. If in fact the micelles are spherical, the slight discrepancy between the radius we calculated and that obtained from light scattering could be due to the locations of the transition dipoles in the micelle. The structure of the chromophore and its finite size suggest that the transition dipole may lie slightly inside the micelle surface. Hence the radius of the chromophore distribution measured by energy transfer would be slightly smaller than the micelle radius obtained by scattering experiments.

In Sec. I we pointed out that theories which presume an infinite volume and an infinite number of chromophores could not accurately describe energy transport observables in many finite volume systems. We verified this on the present system by attempting to fit the data with several infinite volume approaches. First we used the theory of Gochanour, Andersen, and Fayer[2] to calculate G^s assuming that the ODRB was randomly dispersed throughout the solution (not present in higher local concentrations on the micelles). The infinite volume theory predicted much slower energy transfer than that observed in the experiments. G^s for the highest concentration solution [Fig. 5(b)] was calculated to be 0.71 after 5 ns using this infinite volume model. In contrast, the calculated curve in Fig. 5(b) has $G^s = 0.09$ at 5 ns. Clearly, the data indicate that the chromophores must be present at high local concentrations.

We then attempted to fit the data with a model which assumed that the chromophores were associated with micelles and distributed according to a Poisson distribution, as in Sec. II. Instead of using the theory for G^s developed in that section, however, we used the infinite volume theory.[2] (The donor concentration in a micelle with N donors was taken to be βN, and β was adjusted to the best single value for the five concentrations.) The resulting theoretical curves fit the data very poorly. We also tried a variation of this model, where a G^s was used which describes energy transfer on an infinite plane. [The limit of Eq. (7) as $R \rightarrow \infty$ with N/R^2 held constant was used.] The resulting theoretical curves once again fit very poorly. These comparisons demonstrate that detailed understanding and accurate description of energy transport in finite volume systems require specifically tailored statistical mechanical treatments.

V. CONCLUDING REMARKS

Octadecyl rhodamine B in Triton X-100 micelles is an interesting example of a finite volume energy transport system which is readily accessible for experimental study. As in a naturally occurring photosynthetic unit, clustering of the chromophores in a small volume results in highly efficient energy transport. We have presented time resolved experiments which examine the dynamics of the excitation transport. The results can be understood in detail using a treatment which explicitly considers the distribution of chromophores in a finite volume.

The only adjustable parameter in the theoretical analysis of the energy transport data is the radius of the micelle. The radius was found to be 37 ± 2 Å, in good agreement with the literature values obtained by other methods. It has recently been demonstrated theoretically[11] that $G^s(t)$ can be used to study isolated polymer coils and small aggregates in polymer blends in situations not amenable to study by other

methods. The theory and experiments presented here, in addition to describing energy transport in these highly efficient clustered systems, demonstrate that quantitative information about the size of a finite volume system can be obtained from the analysis of excitation transport observables.

ACKNOWLEDGMENTS

We would like to thank Alan Flamberg for helpful discussions. This work was supported by the Department of Energy, Office of Basic Energy Sciences (Grant DE-AT03-82ER12055). In addition, we would like to thank the National Science Foundation (Grant DMR79-20380) for providing and supporting equipment necessary for this research and Stanford University Center for Materials Research (Grant NSF DMR80-20248) for facilities and equipment used in this work. MDF would like to acknowledge the Simon Guggenheim Memorial Foundation for Fellowship support which contributed to this research.

APPENDIX A

The functions below were fit to $h_3(\alpha)$ over the ranges indicated with a relative error of less than 0.5%. The ranges overlap significantly because the algorithm used for the inverse Laplace transform is extremely sensitive to discontinuities. The overlapping ranges allow each time point to be calculated from ϵ values obtained from only one of the following equations:

$$h_3(\alpha) = 0.02(0.47\times 10^{-5}\alpha + 8.2856\alpha^2 + 3.4028\alpha^3 - 57.26\alpha^4), 10^{-4} < \alpha < 0.2,$$

$$h_3(\alpha) = 0.02(0.026\,752 - 0.977\,67\alpha + 20.94\alpha^2 - 65.445\alpha^3 + 82.96\alpha^4 - 38.33\alpha^5), 0.07 < \alpha < 0.7,$$

$$h_3(\alpha) = 0.02(-3.929\,84 + 13.1866\alpha^{1/3} - 12.7476\alpha^{2/3} + 4.151\,78\alpha), 0.3 \leqslant \alpha \leqslant 1.3,$$

$$h_3(\alpha) = 0.013\,62[0.101\,08 + (1 - 0.073\,91\alpha^{-2.0754})^{0.481\,821} \times (0.898\,92)] + 0.001\,972 \times \exp[-(\alpha + 10.937)^2/76.749 - 1.9676/\alpha], \alpha > 0.5.$$

APPENDIX B

We wish to calculate G^s for the orientation dependent transfer rate from G^s for the orientation averaged transfer rate. An approximate solution to this problem is to calculate the exact correction for the two particle term in the density expansion, and then to apply this correction to all terms.[3] This is a reasonable procedure since higher order terms should require approximately the same correction.

For energy transport on a two dimensional plane (the large R limit of the present problem), G^s for the orientation dependent rate can be obtained by replacing R_0^{DD} with $(\gamma_2)^{1/2} R_0^{DD}$ in the expression for G^s for the orientation averaged rate ($\gamma_2 = 0.8468$).[36] For finite R this replacement does not exactly correct the two particle term. However, we found the procedure of replacing R_0^{DD} with $(\gamma_2)^{1/2} R_0^{DD}$ in Eqs. (5) and (7) to be a very accurate method of obtaining G^s for the orientation dependent transfer rate. We tested this approximation (for $N = 2, 3, 5, 9$) against the exact solution obtained by the computer simulation described in Sec. II using the orientation dependent rate. The approximation is essentially exact at short times (± 0.01 for $G^s > 0.75$) and never in error by more than 0.05. Since $R = \mathscr{R}/R_0^{DD}$, we can write this approximation as Eqs. (12) and (13).

[1] S. W. Haan and R. Zwanzig, J. Chem. Phys. **68**, 1879 (1978).
[2] C. R. Gochanour, H. C. Andersen, and M. D. Fayer, J. Chem. Phys. **70**, 4254 (1979).
[3] C. R. Gochanour and M. D. Fayer, J. Phys. Chem. **85**, 1989 (1981).
[4] J. Klafter and R. Silbey, J. Chem. Phys. **72**, 843 (1980).
[5] K. Godzik and J. Jortner, J. Chem. Phys. **72**, 4471 (1980).
[6] D. L. Huber, Phys. Rev. B **20**, 2307, 5333 (1979).
[7] R. F. Loring, H. C. Andersen, and M. D. Fayer, J. Chem. Phys. **76**, 2015 (1982).
[8] R. J. D. Miller, M. Pierre, and M. D. Fayer, J. Chem. Phys. **78**, 5138 (1983).
[9] J. A. Manson and L. H. Sperling, *Polymer Blends and Composites* (Plenum, New York, 1976), p. 77ff.
[10] C. W. Frank, M.-A. Gashgari, P. Chutikamontham, and V. J. Haverly, in *Studies in Physical and Theoretical Chemistry*, edited by A. G. Walton (Elsevier, Amsterdam, 1980), Vol. X, pp. 187–209.
[11] M. D. Ediger and M. D. Fayer, Macromolecules (to be published); G. H. Fredrickson, H. C. Andersen, and C. W. Frank, *ibid.* **16**, 1456 (1983).
[12] G. S. Beddard and G. Porter, Nature **260**, 366 (1976).
[13] K. Sauer, Acc. Chem. Res. **7**, 257 (1978).
[14] G. A. Kenney-Wallace, J. H. Flint, and S. C. Wallace, Chem. Phys. Lett. **32**, 71 (1975).
[15] B. K.-K. Fung and L. Stryer, Biochemistry **17**, 5241 (1978).
[16] Y. Kusumoto and H. Sato, Chem. Phys. Lett. **68**, 13 (1979).
[17] P. K. F. Koglin, D. J. Miller, J. Steinwandel, and M. Hauser, J. Phys. Chem. **85**, 2363 (1981).
[18] L. A. Sklar, M. C. Doody, A. M. Gotto, Jr., and H. J. Pownall, Biochemistry **19**, 1294 (1980).
[19] R. W. Olson, R. F. Loring, and M. D. Fayer, Appl. Opt. **20**, 2934 (1981).
[20] M. D. Ediger and M. D. Fayer, J. Chem. Phys. **78**, 2518 (1983).
[21] Equation (17) in I contains a transcription error. The third term on the right-hand side should not have a 2 in the denominator.
[22] H. Stehfest, Commun. Assoc. Comput. Mach. **13**, 47, 624 (1970).
[23] R. S. Moog, M. D. Ediger, S. G. Boxer, and M. D. Fayer, J. Phys. Chem. **86**, 4694 (1982).
[24] Th. Förster, Ann. Phys. **2**, 55 (1948).
[25] J. N. Demas and G. A. Crosby, J. Phys. Chem. **75**, 991 (1971).
[26] E. D. Cehelnik, K. D. Mielenz, and R. A. Velapoldi, J. Res. Natl. Bur. Stand. A **79**, 1 (1975).
[27] A. von Jena and H. E. Lessing, Chem. Phys. Lett. **78**, 187 (1981).
[28] A. Plückthun and E. A. Dennis, J. Phys. Chem. **85**, 678 (1981).
[29] A. Ray and G. Némethy, J. Phys. Chem. **75**, 804 (1971).
[30] M. Corti and V. Degiorgio, Opt. Commun. **14**, 358 (1975).
[31] H. H. Paradies, J. Phys. Chem. **84**, 599 (1980).
[32] D. R. Lutz, K. A. Nelson, C. R. Gochanour, and M. D. Fayer, Chem. Phys. **58**, 325 (1981).
[33] J. Eisinger, W. E. Blumerg, and R. E. Dale, Ann. N. Y. Acad. Sci. **366**, 155 (1981).
[34] R. J. Robson and E. A. Dennis, J. Phys. Chem. **81**, 1075 (1977).
[35] At higher temperatures there is some disagreement about the molecular weight of Triton X-100 and similar micelles. See Ref. 30 as well as the following: M. Corti and V. Degiorgio, Phys. Rev. Lett. **45**, 1045 (1980); J. Phys. Chem. **85**, 1442 (1981).
[36] G. H. Fredrickson and C. W. Frank, Macromolecules **16**, 1198 (1983).